Psycho-spatially distinct stressors prompt distinct behavioral strategies through a cell type-specific brain circuit

Mehran Ahmadlou[1,2,*], Maria Giannouli[1], Jacqueline F. M. van Vierbergen[1], Tom van Leeuwen[1], Wouter Bloem[1], Janou H. W. Houba[1], Maryam Yasamin Shirazi[1,2], J. Leonie Cazemier[1], Mohit Dubey[3], Fred de Winter[4], J. Alexander Heimel[1,*]

[1] Circuits, Structure and Function Group, Netherlands Institute for Neuroscience, Meibergdreef 47, 1105 BA Amsterdam, Netherlands.

[2] Sainsbury Wellcome Centre for Neural Circuits and Behaviour, University College London, 25 Howland Street, W1T4JG London, United Kingdom.

[3] Department of Axonal Signaling, Netherlands Institute for Neuroscience, Meibergdreef 47, 1105 BA Amsterdam, Netherlands.

[4] Laboratory for Neuroregeneration, Netherlands Institute for Neuroscience, Meibergdreef 47, 1105 BA Amsterdam, Netherlands.

[*] Corresponding author. E-mail: m.ahmadlou@ucl.ac.uk, a.heimel@nin.knaw.nl

Abstract

Selecting the right response to emotional stressors is vital for survival. From the psycho-spatial point of view, the perceived stressors can fall into two conditions: the stressors outside the confined safe zone or inside. Although this novel approach of categorizing the stressors distinguishes two anxiety-associated pathological conditions, agoraphobia and claustrophobia, the difference between the behavioral responses in these two conditions and the underlying brain circuits are not well understood. Here, using novel behavioral paradigms in mice, we found that outside- and inside-stressors elicit two distinct behaviors, push-bedding and escape-jumping, respectively. Next, in an attempt to identify the brain regions activated in both outside- and inside-stressor conditions, the whole-brain c-Fos staining led us to an unexpected brain region, dorsomedial hypothalamus (DMH). Using optogenetics, chemogenetics, and photometry recording, we discovered that glutamatergic projections from DMH to the periaqueductal gray drive the escape to the inside-stressor, while GABAergic projections, in particular from neurons expressing tachykinin 1, are essential for coping with the outside-stressor. We conclude that distinct populations within the DMH region control the response to psycho-spatially distinct stressors. This discovery shows how the stressors and the spatial information of the stressors integrate in the brain and it is the first to shed light on understanding the narrow border between the two space-associated stress disorders/phobias, i.e. agoraphobia and claustrophobia and the underlying brain mechanisms.

From the psycho-spatial point of view, stressors come in two types. When there are stressors outside your safe zone, they can make you feel helpless and trapped (outside-stressor situation). This results in coping behavior. When stressors are inside your safe zone (inside-stressor situation), they result in an active escape-seeking behavior. Understanding mechanisms of the emotional stress induced by these two types and the associated behaviors may uncover the narrow borders between the two space-associated stress disorders, i.e. agoraphobia and claustrophobia. Although rodents are a common model to investigate anxiety-associated disorders, it is unclear whether these two types of emotional stress result in different behavioral strategies in rodents. Understanding this, is a necessary step for understanding the underlying brain mechanism of these disorders. While recent studies have extensively investigated the bottom-up brain circuits for fear responses (e.g. startle freezing and startle running/fleeing) (*1–5*), the top-down brain circuits underlying strategy planning and selection in response to stressors are less well studied (*6*).

Undoubtedly, hypothalamus as the brain controller of the hypothalamic-pituitary-adrenal (HPA) axis plays a key role in stress and fear responses. The dorsomedial hypothalamus (DMH) has long been associated with the regulation of oriented escape, a panic-like defensive response (*7–11*). Accumulating evidence implicates the central role of DMH in inhibiting and driving the HPA axis and integrating physiological and behavioral responses to emotional stressors (*12–16*). Decades of studies, using lesioning and pharmacological experiments have shown that altering the activity of DMH neurons alters both autonomic and behavioral responses to stressors (*17–22*). Recently, Kataoka et al. (2020) showed that emotional stress signaled by prefrontal cortex to the DMH, drives autonomic responses to the emotional stressors. Here, we questioned the role of DMH in stressful situations that differ in the psycho-spatial aspect, either an outside-stressor or an inside-stressor, and whether DMH neurons are differentially involved in the top-down circuits of feeling and expressing the stress responses in the inside-stressor and outside-stressor situations.

First, we developed behavioral tests to investigate behavioral correlates of mice 'feeling' trapped and mice sensing a chance to get out of a stressful environment. Next, after finding cFos expression in the DMH in both these situations, we checked if the situations and responses are distinguishable in DMH. Using optogenetics and calcium fiber photometry, we showed that two separate populations of neurons in the dorsal hypothalamus are essential for these two different emotional states which consequently lead to two different behavioral responses. Finally, we showed that for both behavioral responses the projection of these two neural populations to the key region in the midbrain fear circuit, i.e. periaqueductal gray, is required.

Behavioral responses to inside- and outside-stressors

First, we designed a paradigm where we provide stressors in close proximity to the mouse and allow the mouse a potential escape-route. In this paradigm, the mouse is in a small plexiglass box (with an open top), for ten minutes, where all safe places (i.e. the four corners) have cotton balls with an innately threatful odor of a predator, 2,5-dihydro-2,4,5-trimethylthiazoline (TMT) (*23*) (**Fig. 1A, movie S1**). The results showed a dramatically larger number of jumps compared to the control (without TMT) (**Fig. 1B**). The number of jumps when all corners contained TMT cotton balls was also significantly higher than when mice had safe corner opportunities (**Fig. 1C**). This paradigm provides therefore a situation where the stressors are placed inside the safe zone and provoke robust escape-seeking behavior.

The behavior of mice being trapped in a situation where the threat comes from the outside is yet unclear. In order to find out how mice behave when they feel trapped and helpless in such a situation, we made a paradigm in which the mouse is in an open cage with a thick layer of bedding (to provide an environment similar to its home cage) and we placed cotton balls with TMT directly surrounding the cage (**Fig. 1D**). The mouse could easily leave the cage. We measured well-studied defensive behaviors (jumping, freezing, tail-

rattling), self-grooming, rearing and push-bedding. The latter is the displacement of the bedding by, mostly, the snout and partially by forepaws (**movie S2**). After a short period of exploration (rearing, sniffing the cotton balls), mice sensed the outside-stressor. They showed less grooming and spent much more time inside the cage, compared to the control group where no TMT was placed outside the cage (**Fig. 1, E and F**). Interestingly, mice showed significantly higher duration of push-bedding compared to the control group and no significant change in other defensive behaviors (**Fig. 1G**). The more intense the stressor was, the higher was the duration of the push-bedding behavior (**fig. S1**). Moreover, to see whether the push-bedding is a unique coping behavior specific to being trapped by an outside-stressor or whether it is also evoked in an inside-stressor situation, we placed the TMT cottons inside the cage with bedding (**Fig. 1H**). In this situation, mice did not show push-bedding and they preferred to escape the box (**Fig. 1I**). To test whether the push-bedding behavior occurs only in response to TMT or olfactory stressors and not to other stressors, we trapped the mouse by installing air puffers around the box. Whenever the mouse investigated the possibility to venture out of the cage, it received an air puff (**Fig. 1J, movie S3**). After ten minutes in which the mouse learned of the existence of this outside-stressor, we scored its behavior for ten minutes. Interestingly, again among all fear responses, mice predominantly showed push-bedding behavior and did this for much longer than control animals surrounded by inactive puffers (**Fig. 1K**). This suggests that the push-bedding is not a response that is specific to predator smell but to an outside-stressor in general.

Excitatory neurons in DMH are required for inside-stressor fear response.

The role of DMH in stress and fear responses has been well studied. Recent studies have shown that pharmacologically activating DMH induces defensive alertness behavior and vertical oriented jumping (*11*), which is distinct from the well-studied startle and "explosive" defensive behavior and jumping induced by activating the midbrain defensive circuit (e.g. PAG) (*2*, *4*, *11*). However, it is unknown whether the DMH plays a role in the two psycho-spatially distinct fear responses, i.e. escape jumping instigated by the inside-stressor situation and the push-bedding coping behavior in response to the outside-stressor situation. Our cFos-based brain mapping showed that DMH is indeed one of the few brain regions activated in both inside-stressor and outside-stressor conditions (**fig. S2**).

Next, we questioned whether the DMH is involved differently in these two inside- and outside-stressor situations. One possibility is that activity signaling of fear or stress in general, regardless of the situation, is present in the DMH, and that the differences in behavioral outcome depend on different inputs or processing in downstream areas. Another possibility is that the neural activity is already situation-specific in the DMH. To examine this, we first manipulated excitatory neurons in the DMH.

In order to activate the excitatory neurons in the DMH, we expressed ChR2 bilaterally in DMH of VGluT2-Cre mice through injection of an AAV virus (**Fig. 2A**). Upon activation, mice did not show any push-bedding when they were in the cage with bedding (**Fig. 2B**), but they showed a dramatic increase in the number of jumping in the open field (**Fig. 2C**). They showed no other types of defensive behavior (no freezing, no tail rattling). The induced jumping was not a startle response, but it was a coordinated jump evidenced by a progressive behavior over time (initiated by orienting the head/body, followed by running, making a jumping posture and ending by jumping) (**Fig. 2D, movie S4**). We examined whether the induced jumping is goal-directed, by activating the DMH^{VGluT2} neurons in an open field box with an opening at one of the top corners (**Fig. 2E**). Interestingly, the jumps induced by the photostimulation were tremendously goal-directed towards the top open corner (**Fig. 2F**), and the preference for the corner with the top open was not merely because the mouse was close to that corner when the light was not yet activated (**Fig. 2G**).

These results imply that the photostimulated jumping is a top-down goal-directed behavior which needs integrative processing, rather than a bottom-up startle response.

Furthermore, to test whether the observed jumping was an escape behavior or purely a locomotive behavior, we examined whether the photostimulation induces aversion and negative arousal. Therefore, we optogenetically activated DMH^{VGluT2} neurons in head-fixed mice and video recorded the pupil and whiskers. The pupil size and whisker activity measures showed an increased arousal level by activation of the DMH^{VGluT2} neurons (**Fig. 2, H and I**). The valence was examined using a real-time place preference/avoidance test in a double-chamber, where one of the chambers is linked to the optogenetic light (light-chamber). Compared to control mice which were injected with a tdTomato-vector, activation of the DMH^{VGluT2} neurons significantly decreased the time spent in the light-chamber (**Fig. 2J**). Moreover, one day after two sessions of conditional activation of the DMH^{VGluT2} neurons in the real-time place preference/avoidance test, in the absence of photostimulation, mice spent less time in the light-chamber, indicating the formation of an associative fear memory (**Fig. 2K**). These results together showed that activation of the DMH^{VGluT2} neurons induces a negative arousal commonly associated with fear and stress. Moreover, photostimulation of the DMH^{VGluT2} neurons in presence of their own nesting material (decreasing stress) or cotton balls with TMT (increasing stress), revealed that the number of the induced jumps was modulated by the stressor levels (**fig. S3**).

Next, we questioned whether the DMH^{VGluT2} neurons are necessary for expressing fear of the inside-stressor situation. To answer this, we expressed stGtACR2 in the DMH^{VGluT2} neurons and photo-inhibited them in the inside-TMT paradigm. Interestingly, compared to the tdTomato control mice that also had an optic fiber connected, the jumping behavior was dramatically suppressed (**Fig. 2L**) and there were no other significant stress responses (freezing and tail rattling). Furthermore, photo-inhibition of the DMH^{VGluT2} neurons did not significantly suppress the push-bedding behavior in the outside-stressor paradigm (**Fig. 2M**). Moreover, calcium photometry of GCaMP6s expressed in DMH^{VGluT2} neurons (**Fig. 2N**) showed that these neurons were activated during running/jumping induced by stressors in the inside-stressor situation, but not by push-bedding behavior in the outside-stressor situation (**Fig. 2, O and P**). Therefore, activity of DMH^{VGluT2} neurons is specific for the fear of an inside-stressor and the ensuing response and not for the fear of an outside-stressor and the corresponding response.

Inhibitory neurons in DMH are required for outside-stressor fear response.

It has been shown that DMH is important in the regulation of acute hypertensive and tachycardic responses to mental stress in an air-jet stress paradigm (*12*, *24*). As DMH^{VGluT2} neurons did not influence the fear response to outside-stressor, we asked whether another population of neurons, rather than the excitatory neurons in the DMH plays a role in the outside-stressor fear response. To this end, we targeted the inhibitory neurons in the DMH. In order to activate the inhibitory neurons in the DMH, we expressed ChR2 bilaterally in DMH of GAD2-Cre mice through injection of an AAV virus (**Fig. 3A**). Activation of DMH^{GAD2} neurons did not cause any jumping in the open field (**Fig. 3B**), but dramatically increased push-bedding when the mice were in the cage with bedding (**Fig. 3C**), while there was no significant change in other defensive behaviors (freezing, running, jumping and tail rattling). However, more than VGluT2, GAD2 is expressed in many neurons in nearby brain regions, and there is a risk of the virus spreading into these regions. Knowing that Tachykinin 1 (TAC1), which encodes an important neuropeptide for stress regulation and anxiety-related behavior (*25*, *26*), substance P, is expressed in DMH (https://portal.brain-map.org/) and that substance P in DMH plays a key role in controlling physiological responses to stress, through the HPA axis (*27*), together with the evidence that in some thalamic and subthalamic regions (e.g. thalamic reticular

nucleus, lateral geniculate nucleus and zona incerta) TAC1 is exclusively expressed in inhibitory neurons (*28*, *29*) (https://portal.brain-map.org/), we examined whether TAC1 is also expressed in the DMH inhibitory neurons. Our double-color in-situ hybridization showed that DMH^{TAC1} neurons are inhibitory (**fig. S4 ; Fig. 3D**). Activation of the DMH^{TAC1} neurons (**Fig. 3E**) showed the same results as activation of the encompassing group of inhibitory neurons, i.e. exclusively inducing push-bedding behavior (**Fig. 3F, movie S5**) and not the jumping behavior.

Furthermore, we asked whether activation of the DMH^{TAC1} neurons induces a general state of fear or if it only elicits the push-bedding action. To answer this question, we first examined whether a negative arousal level is increased by activation of the DMH^{TAC1} neurons. Therefore, we optogenetically activated DMH^{TAC1} neurons in head-fixed mice and video recorded the pupil and whiskers. The pupil size and whisker activity measures showed an increased arousal level by activation of the DMH^{TAC1} neurons (**Fig. 3, G and H**). The valence was examined using a real-time place preference/avoidance test in a double-chamber, where one of the chambers is linked to the optogenetic light (light-chamber). Compared to the tdTomato control mice, activation of the DMH^{TAC1} neurons significantly decreased the time spent in the light-chamber (**Fig. 3I**). These results together showed that activation of the DMH^{TAC1} neurons induces a negative arousal that is associated with fear or stress.

In order to see whether the photo-induced fear is associated with an outside-stressor, we placed the mouse in a cage with bedding and its own nesting material for 10 minutes, while the outside surface is elevated to make it as easy as possible for the mouse to explore outside the cage. Activation of the DMH^{TAC1} neurons during the whole period in this paradigm significantly increased the time spent inside the cage compared to the tdTomato control mice (**Fig. 3J**). While the negative valence will be induced by the photo-activation at both locations, the mice thus prefer to do push-bedding in the vicinity of their own nesting material and do not try to escape. The behavior induced by photo-activation of DMH^{TAC1} neurons is thus consistent with the behavior in response to an outside-stressor.

Next, we examined whether repetitively activating the DMH^{TAC1} neurons over days can form an associative fear memory of being trapped by the outside-stressor situation. To achieve this, we first put the mice 10 minutes in a cage with bedding and a visually cued context and measured their behavior. For the next two days the DMH^{TAC1} neurons were photostimulated in the cage for 2 minutes. Next day, we put the mice 10 minutes in the cage without photostimulation and measured their behavior again. The results showed a dramatic increase in push-bedding (and not other fear responses; i.e. freezing, jumping, tail rattling) in the last day compared to the first day (**Fig. 3K**), implying formation of an associative fear memory of being trapped by the outside-stressor situation.

To answer the question whether push-bedding behavior is related to aggression, we photostimulated DMH^{TAC1} neurons in these mice in an open field (without bedding) with intruder conspecifics. Mice showed no aggressive behavior (**fig. S5**), indicating that the push-bedding is not a proactive or defensive aggression. Furthermore, activation of the DMH^{TAC1} neurons decreased the social interactions (**fig. S5**). Moreover, further experiments showed that the behavior induced by the photo-activation is not associated with food and object seeking and running to a nest.

Next, we questioned whether the DMH^{TAC1} neurons are necessary for expressing the fear response to an outside-stressor. To answer this, we expressed stGtACR2 in the DMH^{TAC1} neurons and photo-inhibited them in the outside-TMT paradigm. This intensely suppressed the push-bedding behavior, compared to tdTomato control mice (**Fig. 3L**) and there were no other compensatory stress responses (jumping, freezing, tail-rattling). Furthermore, photo-inhibition of the DMH^{TAC1} neurons did not significantly suppress the number of jumps in the inside-stressor paradigm (**Fig. 3M**). Moreover, calcium photometry of GCaMP6s

expressed in DMH^{TAC1} neurons (**Fig. 3N**) showed that these neurons are activated by stressors in the outside-stressor situation and during push-bedding behavior, but not in the inside-stressor situation and not during running/jumping (**Fig. 3, O and P**). Therefore, the DMH^{TAC1} neurons are specialized for the outside-stressor fear and fear response and not for inside-stressor fear and fear response.

DMH to PAG projections mediate outside and inside-stressor responses.

Periaqueductal gray (PAG) is a key midbrain region in processing the fear response (*2*, *4*). Previous studies have shown that inhibition of PAG neurons or activation of serotonin receptors in PAG reduces the cardiovascular response to emotional stress evoked by the DMH activation (*30*, *31*). Therefore, we examined whether the DMH projection to PAG (*32–34*) also coordinates the responses to the inside- and outside- stressors. Interestingly, our viral tracing experiments showed that lateral PAG receives direct input from both DMH^{TAC1} neurons (**Fig. 4A**) and DMH^{VGluT2} neurons (**Fig. 4B**). Therefore, we asked whether the DMH^{TAC1} → lPAG and DMH^{VGluT2} → lPAG projections contribute to the outside-stressor and inside-stressor fear responses. To answer this, we first expressed ChR2 in DMH^{TAC1} neurons and DMH^{VGluT2} neurons in two groups of mice and optogenetically activated projections of neurons to the lPAG. Photostimulation of the DMH^{TAC1} → lPAG and DMH^{VGluT2} → lPAG showed a significant increase in the push-bedding (**Fig. 4C**) and jumping (**Fig. 4D**) behaviors, respectively. Next, we investigated whether these projections are necessary for the outside-stressor and inside-stressor fear responses. In order to test this, using AAV-DIO-hM4Di and local injection of CNO in lPAG, we chemogenetically suppressed the DMH^{TAC1} → lPAG and DMH^{VGluT2} → lPAG axons. Inhibition of DMH^{TAC1} → lPAG axons showed a dramatic reduction of push-bedding in the outside-stressor TMT paradigm (**Fig. 4E**). Inhibition of DMH^{VGluT2} → lPAG axons showed an intensive decrease in jumping behavior in the inside-stressor TMT paradigm (**Fig. 4F**). We conclude that different projections from the DMH to the lPAG drive the response to both inside- and outside-stressors.

Agoraphobia and claustrophobia are manifestations of two distinct psycho-spatial associated anxieties, anxiety from outside our psychologically safe place (e.g. home) and anxiety of being trapped in a small place (e.g. an elevator), respectively. The behavioral read-out of these two psycho-spatial associated anxieties in non-human animals is not well-studied. Using novel behavioral paradigms, we discovered that mice elicit two distinct anxiety responses in the outside-stressor and inside-stressor tests, i.e. push-bedding and escape jumping, respectively. This finding enabled us to investigate the brain circuits associated with the responses to these two psycho-spatial distinct sources of anxiety. Surprisingly, we found that two distinct neuronal populations (GABAergic and glutamatergic neurons), in the same brain region, DMH, a central driver of emotional stress responses (*15*), differentially drive the anxiety associated responses to the outside- and inside- stressors. Moreover, we found that the GABAergic DMH→PAG projection is required for the outside-stressor response, push-bedding, and the glutamatergic DMH→PAG projection is required for the inside-stressor response, escape jumping.

In this study, we did not investigate the upstream circuit. However, differentiating these two situations, sensing the outside and inside stressors, needs integration of sensory information and a top-down control resulting from the perceptual differentiation. Interestingly, DMH receives a predominant input from the ventromedial prefrontal cortex (vmPFC; **fig. S6**) (*35*, *36*) which is known to exert top-down control over subcortical structures, such as DMH, to regulate anxiety-associated behavioral responses (*35*). A recent study showed that an excitatory projection from specific areas of vmPFC to DMH drives autonomic responses to emotional (more specifically psychosocial) stress (*15*). Therefore, we hypothesize that vmPFC

input to DMH sends the perceptually differentiated signals associated with the outside- and inside- stressor situations to select appropriate behavioral responses. Paraventricular nucleus of hypothalamus (PVN) receives a prominent glutamatergic, GABAergic and interestingly substance P input from DMH (*27*, *37*, *38*), which could potentially induce autonomic stress responses associated with agoraphobia and claustrophobia. Therefore, we hypothesize that in parallel to the DMH→PAG pathway to execute the associated behavioral responses, the DMH→PVN projections may differentially induce autonomic stress responses associated with agoraphobia and claustrophobia. Further studies need to examine the aforementioned hypotheses.

Acknowledgements

We thank Mejdy Kacem, Andres de Groot, Ralph Hamelink, Maurice Heemskerk, Martin Oomstee, Stephen Super, John van Veldhuijzen, Marian Verhage, Nanneke van der Wal, Joris Coppens and Joost Verhaagen. **Funding:** This work was supported by the Dr. J.L. Dobberke Foundation. **Author contributions:** M.A. conceived the study with input from J.A.H. M.A., M.G., J.F.M.v.V., T.v.L., W.B., J.H.W.H., M.Y.S., J.L.C., M.D., M.H.P.K. and J.A.H. collected and analyzed the data. F.d.W. made viral vectors and helped the in situ hybridization. M.A. and J.A.H. wrote the paper. **Competing interests:** Authors declare no competing interests. **Data and materials availability:** All behavioral movies and scripts are stored on institutional storage and are available upon request from the authors.

Fig 1. Behavioral fingerprints for "being in an inside-stressor situation" and "being trapped in an outside-stressor situation".

(**A**) Schematics of an inside-stressor test with TMT cottons located at all corners. (**B**) Bar graph shows the number of jumps taken by C57BL/6 mice in the inside-stressor test without (N = 10 mice) and with TMT (N = 5 mice). (**C**) Schematics of the inside-stressor test with TMT cottons located at 1, 2, 3 and 4 corners. Bar graph shows the number of jumps taken by C57BL/6 mice in the inside-stressor test with 1, 2, 3 and 4 corners filled with TMT cotton (N = 5, 5, 5 and 10 mice, respectively). (**D**) Schematics of an outside-stressor test with TMT cottons sticking at all edges outside the home-like cage with a thick layer of beddings. (**E**) Bar graph shows duration of self-grooming without (N = 12 mice) and with (N = 9 mice) TMT. (**F**) Bar graph of duration of time spent outside the cage (defined by all paws and body lifted up from the bedding surface) without and with TMT in C57BL/6 mice (N = 10 and 8 mice, respectively). (**G**) Stacked bar graph shows duration for each action (push-bedding, self-grooming, rearing, jumping, tail rattling and freezing) in the outside-stressor test (without and with TMT) taken by the mice in (E). The bar graph shows duration of push-bedding in the outside-stressor test without and with TMT taken by the mice in (E). (**H**) Schematics of an inside-stressor test with TMT cottons located at all corners inside the home-like cage with a thick layer of bedding. (**I**) Stacked bar graph shows duration of the actions (push-bedding, self-grooming, rearing, jumping, tail rattling and freezing) when the TMT cottons are outside or inside the cage, normalized by the duration of time spent inside the cage. The bar graph shows the duration of time spent outside the cage when the TMT cottons are outside or inside the cage (N = 8 and 7 mice, respectively). (**J**) Schematics of an outside-stressor test with air puff holes located at all edges outside the home-like cage with a thick layer of bedding. In the 10-min period prior to the test, mice receive air puffs upon sniffing the air puff holes. The behavioral response is measured in the next 10 minutes without the exposure to the air puff. (**K**) Stacked bar graph shows duration of the actions (push-bedding, self-grooming, rearing, jumping, tail rattling and freezing) without (control) and with air puff prior to the test. The bar graph shows the duration of push-bedding in both conditions (N = 5 and 6 mice, respectively).

Fig 2. Excitatory neurons in DMH are required for inside-stressor fear response.
(**A**) Expression of AAV-ChR2-mCherry in DMH of a VGluT2-Cre mouse. Scale bar indicates 0.25 mm. (**B**) Schematics of photo stimulation of DMH^{VGluT2} neurons in the home-like cage with beddings (without TMT). The bar graph shows the number of push-bedding occurrences by each photo stimulation normalized to the number of photo stimulation trials (in percentage) in tdTomato and ChR2 injected mice (N = 5 and 4 mice, respectively). (**C**) Schematics of photo stimulation of DMH^{VGluT2} neurons in the box (without TMT). The bar graph shows the number of jumps by each photo stimulation normalized to the number of photo stimulation trials (in percentage) in tdTomato and ChR2 injected mice (N = 5 and 14 mice, respectively). (**D**) Transition probability between the measured actions (alertness (sudden head/body orienting), run, posture (posture preparation for jumping), jump and the onset of photo stimulation of the DMH^{VGluT2} neurons with different durations of photo stimulation (N = 20 trials per photo stimulation duration, 3 mice). The color bar indicates probabilities between 0.01 and 1. Transition probability less than 0.01 is shown with no edge between the nodes, for better visualization. (**E**) Schematics of photo stimulation of DMH^{VGluT2} neurons in the box (without TMT) with a hole in one top corner (corner hole). (**F**) The bar graph shows the number of jumps to each of the top corners by each photo stimulation normalized to the number of photo stimulation trials (in percentage) in ChR2 injected mice (N = 5 mice). (**G**) Histogram of number of jumps to the corner hole as a function of normalized distance (at the start of the photo stimulation) to the corner hole in mice of (F). The bar graph shows the number of jumps to the nearest top corner and the corner hole after each photo stimulation normalized to the number of photo stimulation trials (in percentage). (**H**) Z-score (middle) and mean Z-score (right) of pupil size of tdTom (red; N = 7 mice) and ChR2 (blue; N = 5 mice) mice with photo stimulation from 0 to 5 s. (**I**) Z-score (middle) and mean Z-score (right) of whisker activity of mice in (H). (**J**) An example heatmap of the track of a ChR2 mouse in a real time place preference/aversion (RTPPA) test. The bar graph shows the duration of time that control tdTom and ChR2 (N = 6 and 6 mice, respectively) mice spent in the opto-linked chamber in the RTPPA test. (**K**) Schematics of the RTPPA conditioning test, where ChR2 mice on day 2 and day 3 are photo stimulated in one chamber (the preferred chamber in the pre-conditioning day). On day 1, pre-conditioning, and day 4, post-conditioning, there is no photo stimulation. The bar graph shows duration of time spent in the preferred chamber before and after conditioning (N = 6 mice). The red dashed line represent the chance level (50%). The duration after conditioning is significantly lower than chance level (T-test; p-value: 0.0003, $t[6] = 7.4488$). (**L**) Schematics of photo inhibition of DMH^{VGluT2} neurons in the inside-stressor test with the TMT cottons. The bar graph shows the number of jumps (in the 10-min test) in tdTomato and stGtACR2 injected mice (N = 6 and 5 mice, respectively). (**M**) Schematics of photo inhibition of DMH^{VGluT2} neurons in the home-like cage with beddings with outside-stressor (TMT). The bar graph shows the duration of push-bedding (in the 10-min test) in tdTomato and stGtACR2 injected mice (N = 5 and 5 mice, respectively). (**N**) Schematic of calcium photometry of DMH^{VGluT2} neurons in inside- and outside-stressor tests. (**O**) Calcium activity of DMH^{VGluT2} neurons (dF/F0 Z-score) in inside- (green) and outside-stressor (orange) tests, averaged over trials. The light color around the average indicates the standard error. Time 0 s in inside-stressor test is the onset of running away (or running + jumping) and in outside-stressor test is the onset of push-bedding. (**P**) Mean Z-score of calcium activity in response to stressors in outside- and inside-stressor tests (N = 47 and 82 events, 4 mice, respectively).

Fig 3. Inhibitory neurons in DMH are required for outside-stressor fear response.
(**A**) Expression of AAV-ChR2-mCherry in DMH of a GAD2-Cre mouse. Scale bar indicates 0.2 mm. (**B**) Schematics of photo stimulation of DMH^{GAD2} neurons in the box (without TMT). The bar graph shows the number of jumps by each photo stimulation normalized to the number of photo stimulation trials (in percentage) in tdTomato and ChR2 injected mice (N = 5 and 3 mice, respectively). (**C**) Schematics of photo stimulation of DMH^{GAD2} neurons in the home-like cage with beddings (without TMT). The bar graph shows the number of push-bedding occurrences by each photo stimulation normalized to the number of photo stimulation trials (in percentage) in tdTomato and ChR2 injected mice (N = 5 and 4 mice, respectively). (**D**) Example of a double-color in-situ mRNA hybridization in DMH. DAPI is shown in blue and TAC1+ and VGAT+ cells are in green and red, respectively. The bottom right panel shows the overlap between the three colors. Scale bar indicates 0.1 mm. (**E**) Expression of AAV-ChR2-mCherry in DMH of a TAC1-Cre mouse. Scale bar indicates 0.1 mm. (**F**) Stacked bar graph shows duration for each action (push-bedding, self-grooming, rearing, jumping, tail rattling and freezing) in the home-like cage with beddings (without TMT) in photo stimulated tdTomato and ChR2 TAC1-Cre mice. The bar graph shows the number of push-bedding occurrences by each photo stimulation normalized to the number of photo stimulation trials (in percentage) (N = 5 and 12 mice, respectively). (**G**) Z-score (left) and mean Z-score (right) of pupil size of tdTom (red; N =5 mice) and ChR2 (blue; N = 5 mice) mice with photo stimulation from 0 to 5 s. (**H**) Z-score (left) and mean Z-score (right) of whisker activity of mice in (F). (**I**) An example heatmap of the track of a ChR2 TAC1-Cre mouse in a real time place preference/aversion (RTPPA) test. The bar graph shows the duration of time that control tdTom and ChR2 (N = 8 and 8 mice, respectively) mice spent in the opto-linked chamber in the RTPPA test. (**J**) Schematics of photo stimulation of DMH^{TAC1} neurons in the home-like cage with their own nesting material inside the cage and beddings both inside the cage and outside the cage, on an elevated platform around the cage, to facilitate traveling between inside and outside the cage and to make equal possibility of push-bedding behavior in both sides. Mice are photo stimulated all the time (with random time intervals between the pulses), both inside and outside the cage. The bar graph shows the percentage of time spent inside the cage in tdTomato and ChR2 mice (N = 5 and 5, respectively). (**K**) Schematics of the photo stimulation conditioning test, where ChR2 mice on day 2 and day 3 are photo stimulated in the home-like cage. On day 1, pre-conditioning, and day 4, post-conditioning, there is no photo stimulation. The bar graph shows duration of push-bedding before and after conditioning (N = 5 mice). (**L**) Schematics of photo inhibition of DMH^{TAC1} neurons in the outside-stressor test with the TMT cottons. The bar graph shows the duration of push-bedding in tdTomato and stGtACR2 injected mice (N = 6 and 5 mice, respectively). (**M**) Schematics of photo inhibition of DMH^{TAC1} neurons in the inside-stressor test with the TMT cottons. The bar graph shows the number of jumps in tdTomato and stGtACR2 injected mice (N = 5 and 5 mice, respectively). (**N**) Schematic of calcium photometry of DMH^{TAC1} neurons in inside- and outside-stressor tests. (**O**) Calcium activity of DMH^{TAC1} neurons (dF/F0 Z-score) in inside- (green) and outside-stressor (orange) tests, averaged over trials. The light color around the average indicates the standard error. Time 0 s in inside-stressor test is the onset of running away (or running + jumping) and in outside-stressor test is the onset of push-bedding. (**P**) Mean Z-score of calcium activity in response to stressors in outside- and inside-stressor tests (N = 45 and 104 events, 4 mice, respectively).

Fig 4. Outside-stressor and inside-stressor responses are controlled through distinct DMH to PAG projections.

(**A**) Expression of AAV-ChR2-mCherry in DMH^{TAC1} axons in lPAG. Scale bar indicates 0.25 mm. (**B**) Expression of AAV-ChR2-mCherry in DMH^{VGluT2} axons in lPAG. Scale bar indicates 0.25 mm. (**C**) Schematics of photo stimulation of DMH^{TAC1} axons in lPAG in the home-like cage with beddings (without TMT). The bar graph shows the number of push-bedding occurrences by each photo stimulation normalized to the number of photo stimulation trials (in percentage) in tdTomato and ChR2 injected mice (N = 6 and 5 mice, respectively). (**D**) Schematics of photo stimulation of DMH^{VGluT2} axons in lPAG in the box (without TMT). The bar graph shows the number of jumps by each photo stimulation normalized to the number of photo stimulation trials (in percentage) in tdTomato and ChR2 injected mice (N = 5 and 4 mice, respectively). (**E**) Schematics of chemogenetic inhibition of DMH^{TAC1} axons in lPAG in the outside-stressor test with TMT. The bar graph shows the duration of push-bedding in mice with local injection of saline and CNO in lPAG (N = 5 and 5 mice, respectively). (**F**) Schematics of chemogenetic inhibition of DMH^{VGluT2} axons in lPAG in the inside-stressor test with TMT. The bar graph shows the number of jumps in mice with local injection of saline and CNO in lPAG (N = 3 and 5 mice, respectively).

References and Notes

1. C. Shang, Z. Liu, Z. Chen, Y. Shi, Q. Wang, S. Liu, D. Li, P. Cao, A parvalbumin-positive excitatory visual pathway to trigger fear responses in mice. *Science (80-.).* **348**, 1472–1477 (2015).
2. D. A. Evans, V. Stempel, R. Vale, S. Ruehle, Y. Lefler, T. Branco, A synaptic threshold mechanism for computing escape decisions. *bioRxiv*, 272492 (2018).
3. T. Kim, N. Shen, J. C. Hsiang, K. P. Johnson, D. Kerschensteiner, Dendritic and parallel processing of visual threats in the retina control defensive responses. *Sci. Adv.* **6** (2020), doi:10.1126/sciadv.abc9920.
4. Y. Lefler, D. Campagner, T. Branco, The role of the periaqueductal gray in escape behavior. *Curr. Opin. Neurobiol.* **60** (2020), , doi:10.1016/j.conb.2019.11.014.
5. M. Niu, A. Kasai, M. Tanuma, K. Seiriki, H. Igarashi, T. Kuwaki, K. Nagayasu, K. Miyaji, H. Ueno, W. Tanabe, K. Seo, R. Yokoyama, J. Ohkubo, Y. Ago, M. Hayashida, K. I. Inoue, M. Takada, S. Yamaguchi, T. Nakazawa, S. Kaneko, H. Okuno, A. Yamanaka, H. Hashimoto, Claustrum mediates bidirectional and reversible control of stress-induced anxiety responses. *Sci. Adv.* **8** (2022), doi:10.1126/sciadv.abi6375.
6. B. J. Fung, S. Qi, D. Hassabis, N. Daw, D. Mobbs, Slow escape decisions are swayed by trait anxiety. *Nat. Hum. Behav.* **3** (2019), , doi:10.1038/s41562-019-0595-5.
7. J. O. G. Nascimento, H. Zangrossi, M. B. Viana, Effects of reversible inactivation of the dorsomedial hypothalamus on panic-and anxiety-related responses in rats. *Brazilian J. Med. Biol. Res.* **43** (2010), doi:10.1590/S0100-879X2010007500075.
8. M. S. C. F. Silva, B. A. Pereira, I. C. Céspedes, J. O. G. Nascimento, J. C. Bittencourt, M. B. Viana, Dorsomedial hypothalamus CRF type 1 receptors selectively modulate inhibitory avoidance responses in the elevated T-maze. *Behav. Brain Res.* **271**, 249–257 (2014).
9. V. C. De Bortoli, P. S. D. M. Yamashita, H. Zangrossi, 5-HT1A and 5-HT2A receptor control of a panic-like defensive response in the rat dorsomedial hypothalamic nucleus. *J. Psychopharmacol.* **27** (2013), doi:10.1177/0269881113492900.
10. F. Ullah, T. dos Anjos-Garcia, I. R. dos Santos, A. F. Biagioni, N. C. Coimbra, Relevance of dorsomedial hypothalamus, dorsomedial division of the ventromedial hypothalamus and the dorsal periaqueductal gray matter in the organization of freezing or oriented and non-oriented escape emotional behaviors. *Behav. Brain Res.* **293**, 143–152 (2015).
11. A. F. Biagioni, T. dos Anjos-Garcia, F. Ullah, I. R. Fisher, L. L. Falconi-Sobrinho, R. L. de Freitas, T. T. Felippotti, N. C. Coimbra, Neuroethological validation of an experimental apparatus to evaluate oriented and non-oriented escape behaviours: Comparison between the polygonal arena with a burrow and the circular enclosure of an open-field test. *Behav. Brain Res.* **298**, 65–77 (2016).
12. E. H. Stotz-Potter, L. R. Willis, J. A. DiMicco, Muscimol acts in dorsomedial but not paraventricular hypothalamic nucleus to suppress cardiovascular effects of stress. *J. Neurosci.* **16**, 1173–1179 (1996).
13. K. Ebner, P. Muigg, N. Singewald, Inhibitory Function of the Dorsomedial Hypothalamic Nucleus on the Hypothalamic-Pituitary-Adrenal Axis Response to an Emotional Stressor but not Immune Challenge. *J. Neuroendocrinol.* **25**, 48–55 (2013).
14. E. Bondarenko, M. I. Beig, D. M. Hodgson, V. A. Braga, E. Nalivaiko, Blockade of the dorsomedial hypothalamus and the perifornical area inhibits respiratory responses to arousing and stressful stimuli. *Am. J. Physiol. - Regul. Integr. Comp. Physiol.* **308**, R816–R822 (2015).
15. N. Kataoka, Y. Shima, K. Nakajima, K. Nakamura, A central master driver of psychosocial stress responses in the rat. *Science (80-.).* **367**, 1105–1112 (2020).
16. K. Nakamura, Y. Nakamura, N. Kataoka, A hypothalamomedullary network for physiological responses to environmental stresses. *Nat. Rev. Neurosci.* **23** (2022), , doi:10.1038/s41583-021-00532-x.

17. R. P. Soltis, J. A. DiMicco, GABA(A) and excitatory amino acid receptors in dorsomedial hypothalamus and heart rate in rats. *Am. J. Physiol. - Regul. Integr. Comp. Physiol.* **260** (1991), doi:10.1152/ajpregu.1991.260.1.r13.
18. A. Shekhar, GABA receptors in the region of the dorsomedial hypothalamus of rats regulate anxiety in the elevated plus-maze test. I. Behavioral measures. *Brain Res.* **627**, 9–16 (1993).
19. J. R. Inglefield, S. B. Schwarzkopf, C. K. Kellogg, Alterations in behavioral responses to stressors following excitotoxin lesions of dorsomedial hypothalamic regions. *Brain Res.* **633**, 151–161 (1994).
20. S. M. Morin, E. H. Stotz-Potter, J. A. Dimicco, Injection of muscimol in dorsomedial hypothalamus and stress-induced Fos expression in paraventricular nucleus. *Am. J. Physiol. - Regul. Integr. Comp. Physiol.* **280**, 1276–1284 (2001).
21. P. J. Gasser, C. A. Lowry, M. Orchinik, Corticosterone-sensitive monoamine transport in the rat dorsomedial hypothalamus: Potential role for organic cation transporter 3 in stress-induced modulation of monoaminergic neurotransmission. *J. Neurosci.* **26**, 8758–8766 (2006).
22. J. L. Hunt, D. V. Zaretsky, S. Sarkar, J. A. DiMicco, Dorsomedial hypothalamus mediates autonomic, neuroendocrine, and locomotor responses evoked from the medial preoptic area. *Am. J. Physiol. - Regul. Integr. Comp. Physiol.* **298**, 130–140 (2010).
23. J. B. Rosen, A. Asok, T. Chakraborty, The smell of fear: Innate threat of 2,5-dihydro-2,4,5-trimethylthiazoline, a single molecule component of a predator odor. *Front. Neurosci.* **9** (2015), , doi:10.3389/fnins.2015.00292.
24. R. De Matteo, G. A. Head, D. N. Mayorov, Tempol in the dorsomedial hypothalamus attenuates the hypertensive response to stress in rabbits. *Am. J. Hypertens.* **19**, 396–402 (2006).
25. K. Ebner, N. Singewald, "The role of substance P in stress and anxiety responses" in *Amino Acids* (2006), vol. 31.
26. K. Iftikhar, A. Siddiq, S. G. Baig, S. Zehra, Substance P: A neuropeptide involved in the psychopathology of anxiety disorders. *Neuropeptides.* **79** (2020), , doi:10.1016/j.npep.2019.101993.
27. M. D. Womack, R. Barrett-Jolley, Activation of paraventricular nucleus neurones by the dorsomedial hypothalamus via a tachykinin pathway in rats. *Exp. Physiol.* **92**, 671–676 (2007).
28. Y. Li, V. G. Lopez-Huerta, X. Adiconis, K. Levandowski, S. Choi, S. K. Simmons, M. A. Arias-Garcia, B. Guo, A. Y. Yao, T. R. Blosser, R. D. Wimmer, T. Aida, A. Atamian, T. Naik, X. Sun, D. Bi, D. Malhotra, C. C. Hession, R. Shema, M. Gomes, T. Li, E. Hwang, A. Krol, M. Kowalczyk, J. Peça, G. Pan, M. M. Halassa, J. Z. Levin, Z. Fu, G. Feng, Distinct subnetworks of the thalamic reticular nucleus. *Nature.* **583** (2020), doi:10.1038/s41586-020-2504-5.
29. M. Ahmadlou, J. H. W. Houba, J. F. M. van Vierbergen, M. Giannouli, G. A. Gimenez, C. van Weeghel, M. Darbanfouladi, M. Y. Shirazi, J. Dziubek, M. Kacem, F. de Winter, J. A. Heimel, A cell type–specific cortico-subcortical brain circuit for investigatory and novelty-seeking behavior. *Science (80-.).* **372** (2021), doi:10.1126/science.abe9681.
30. L. G. Da Silva, R. C. Alvim De Menezes, R. A. Souza dos Santos, M. J. Campagnole-Santos, M. A. Peliky Fontes, Role of periaqueductal gray on the cardiovascular response evoked by disinhibition of the dorsomedial hypothalamus. *Brain Res.* **984**, 206–214 (2003).
31. D. C. Villela, L. G. da Silva Junior, M. A. P. Fontes, Activation of 5-HT receptors in the periaqueductal gray attenuates the tachycardia evoked from dorsomedial hypothalamus. *Auton. Neurosci. Basic Clin.* **148** (2009), doi:10.1016/j.autneu.2009.02.004.
32. G. J. T. Horst, P. G. M. Luiten, The projections of the dorsomedial hypothalamic nucleus in the rat. *Brain Res. Bull.* **16** (1986), doi:10.1016/0361-9230(86)90038-9.
33. R. H. Thompson, N. S. Canteras, L. W. Swanson, Organization of projections from the dorsomedial nucleus of the hypothalamus: A PHA-L study in the rat. *J. Comp. Neurol.* **376** (1996), doi:10.1002/(SICI)1096-9861(19961202)376:1<143::AID-CNE9>3.0.CO;2-3.
34. K. C. G. de Git, D. C. van Tuijl, M. C. M. Luijendijk, I. G. Wolterink-Donselaar, A. Ghanem, K. K. Conzelmann, R. A. H. Adan, Anatomical projections of the dorsomedial hypothalamus to the periaqueductal grey and their role in thermoregulation: a cautionary note. *Physiol. Rep.* **6**, 1–16

(2018).
35. S. J. McDougall, R. E. Widdop, A. J. Lawrence, Medial prefrontal cortical integration of psychological stress in rats. *Eur. J. Neurosci.* **20** (2004), doi:10.1111/j.1460-9568.2004.03707.x.
36. T. F. Giustino, S. Maren, The role of the medial prefrontal cortex in the conditioning and extinction of fear. *Front. Behav. Neurosci.* **9** (2015), , doi:10.3389/fnbeh.2015.00298.
37. W. E. Cullinan, D. R. Ziegler, J. P. Herman, Functional role of local GABAergic influences on the HPA axis. *Brain Struct. Funct.* **213** (2008), , doi:10.1007/s00429-008-0192-2.
38. Y. M. Ulrich-Lai, K. R. Jones, D. R. Ziegler, W. E. Cullinan, J. P. Herman, Forebrain origins of glutamatergic innervation to the rat paraventricular nucleus of the hypothalamus: Differential inputs to the anterior versus posterior subregions. *J. Comp. Neurol.* **519** (2011), doi:10.1002/cne.22571.
39. M. Mahn, L. Gibor, P. Patil, K. Cohen-Kashi Malina, S. Oring, Y. Printz, R. Levy, I. Lampl, O. Yizhar, High-efficiency optogenetic silencing with soma-targeted anion-conducting channelrhodopsins. *Nat. Commun.* **9** (2018), doi:10.1038/s41467-018-06511-8.
40. T.-W. Chen, T. J. Wardill, Y. Sun, S. R. Pulver, S. L. Renninger, A. Baohan, E. R. Schreiter, R. A. Kerr, M. B. Orger, V. Jayaraman, L. L. Looger, K. Svoboda, D. S. Kim, Ultrasensitive fluorescent proteins for imaging neuronal activity. *Nature*. **499**, 295–300 (2013).
41. M. Kabra, A. A. Robie, M. Rivera-Alba, S. Branson, K. Branson, JAABA: Interactive machine learning for automatic annotation of animal behavior. *Nat. Methods*. **10** (2013), doi:10.1038/nmeth.2281.
42. S. Berg, D. Kutra, T. Kroeger, C. N. Straehle, B. X. Kausler, C. Haubold, M. Schiegg, J. Ales, T. Beier, M. Rudy, K. Eren, J. I. Cervantes, B. Xu, F. Beuttenmueller, A. Wolny, C. Zhang, U. Koethe, F. A. Hamprecht, A. Kreshuk, ilastik: interactive machine learning for (bio)image analysis. *Nat. Methods*. **16** (2019), doi:10.1038/s41592-019-0582-9.
43. J. H. Song, W. Choi, Y. H. Song, J. H. Kim, D. Jeong, S. H. Lee, S. B. Paik, Precise Mapping of Single Neurons by Calibrated 3D Reconstruction of Brain Slices Reveals Topographic Projection in Mouse Visual Cortex. *Cell Rep.* **31** (2020), doi:10.1016/j.celrep.2020.107682.
44. M. Ahmadlou, J. A. Heimel, Preference for concentric orientations in the mouse superior colliculus. *Nat. Commun.* **6** (2015), doi:10.1038/ncomms7773.
45. J. P. Sommeijer, M. Ahmadlou, M. H. Saiepour, K. Seignette, R. Min, J. A. Heimel, C. N. Levelt, Thalamic inhibition regulates critical-period plasticity in visual cortex and thalamus. *Nat. Neurosci.* **20**, 1716–1721 (2017).
46. M. Ahmadlou, L. S. Zweifel, J. A. Heimel, Functional modulation of primary visual cortex by the superior colliculus in the mouse. *Nat. Commun.* **9** (2018), doi:10.1038/s41467-018-06389-6.

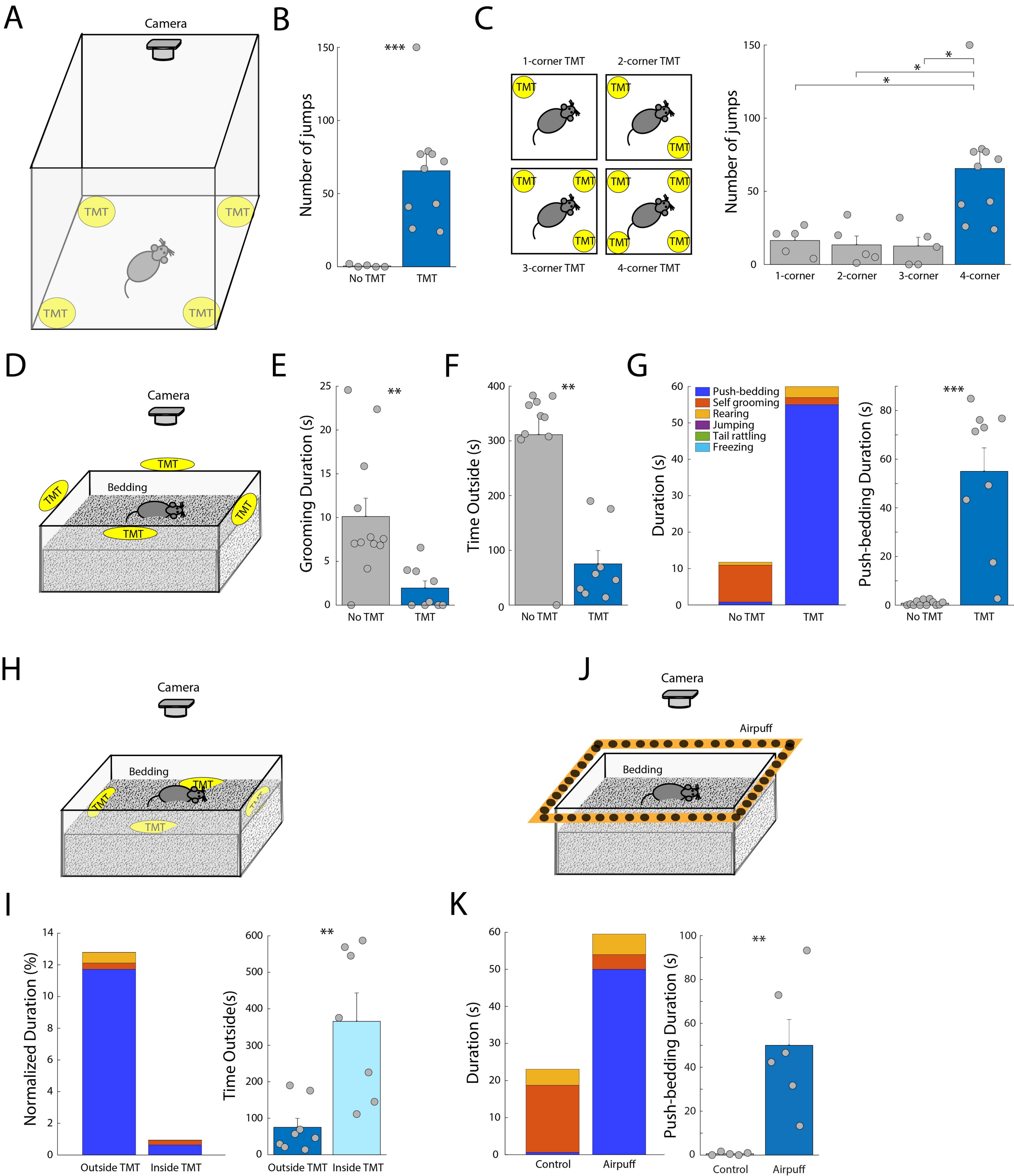
A
Camera
TMT
TMT
TMT
TMT
B
Number of jumps
150
100
50
0
***
No TMT
TMT
C
1-corner TMT
2-corner TMT
3-corner TMT
4-corner TMT
TMT
Number of jumps
150
100
50
0
*
*
*
1-corner
2-corner
3-corner
4-corner
D
Camera
TMT
Bedding
TMT
TMT
TMT
E
Grooming Duration (s)
25
20
15
10
5
0
**
No TMT
TMT
F
Time Outside (s)
400
300
200
100
0
**
No TMT
TMT
G
Duration (s)
60
50
40
30
20
10
0
Push-bedding
Self grooming
Rearing
Jumping
Tail rattling
Freezing
No TMT
TMT
Push-bedding Duration (s)
80
60
40
20
0
***
No TMT
TMT
H
Camera
Bedding
TMT
TMT
TMT
TMT
I
Normalized Duration (%)
14
12
10
8
6
4
2
0
Outside TMT
Inside TMT
Time Outside(s)
600
500
400
300
200
100
0
**
Outside TMT
Inside TMT
J
Camera
Airpuff
Bedding
K
Duration (s)
60
50
40
30
20
10
0
Control
Airpuff
Push-bedding Duration (s)
100
80
60
40
20
0
**
Control
Airpuff

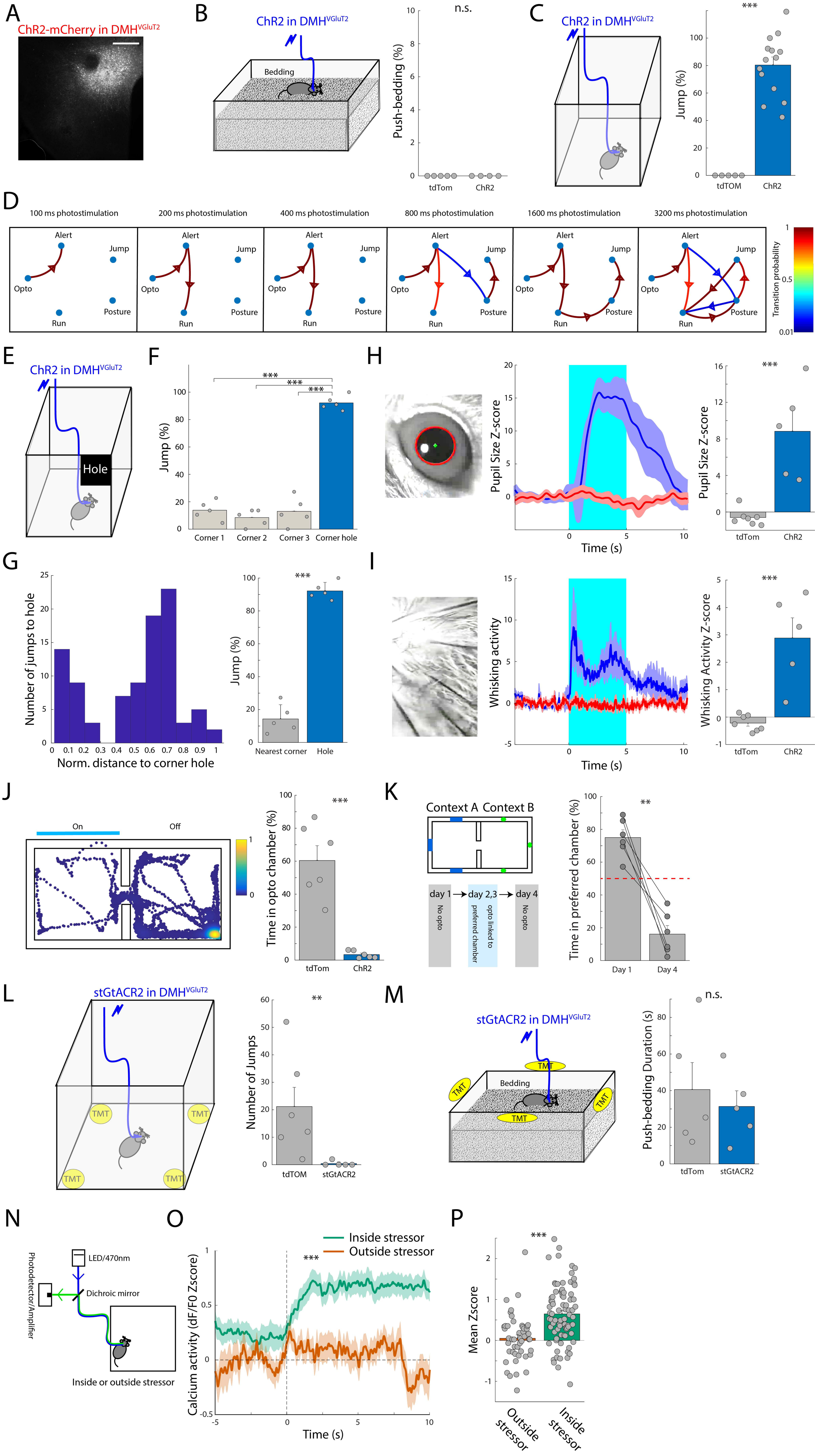
A
ChR2-mCherry in DMH^VGluT2
B
ChR2 in DMH^VGluT2
Bedding
Push-bedding (%)
n.s.
tdTom
ChR2
C
ChR2 in DMH^VGluT2
Jump (%)
***
tdTOM
ChR2
D
100 ms photostimulation
200 ms photostimulation
400 ms photostimulation
800 ms photostimulation
1600 ms photostimulation
3200 ms photostimulation
Alert
Jump
Opto
Posture
Run
Transition probability
E
ChR2 in DMH^VGluT2
Hole
F
Jump (%)
Corner 1
Corner 2
Corner 3
Corner hole
H
Pupil Size Z-score
Time (s)
tdTom
ChR2
G
Number of jumps to hole
Norm. distance to corner hole
Jump (%)
Nearest corner
Hole
I
Whisking activity
Whisking Activity Z-score
Time (s)
tdTom
ChR2
J
On
Off
Time in opto chamber (%)
tdTom
ChR2
K
Context A
Context B
day 1
day 2,3
day 4
No opto
opto linked to preferred chamber
No opto
Time in preferred chamber (%)
Day 1
Day 4
L
stGtACR2 in DMH^VGluT2
TMT
Number of Jumps
tdTOM
stGtACR2
M
stGtACR2 in DMH^VGluT2
TMT
Bedding
Push-bedding Duration (s)
n.s.
tdTom
stGtACR2
N
Photodetector/Amplifier
LED/470nm
Dichroic mirror
Inside or outside stressor
O
Inside stressor
Outside stressor
Calcium activity (dF/F0 Zscore)
Time (s)
P
Mean Zscore
Outside stressor
Inside stressor

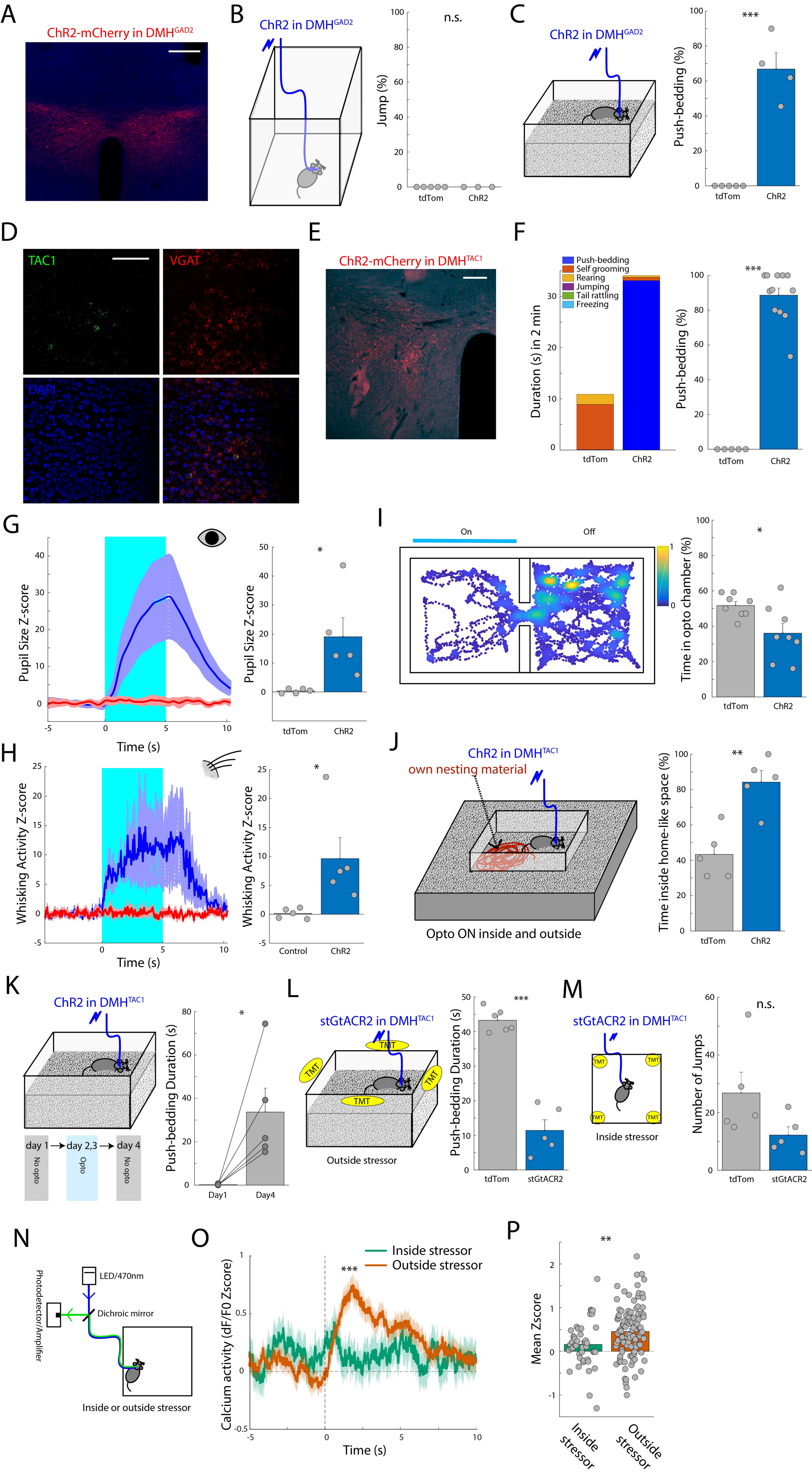
A
ChR2-mCherry in DMH^GAD2
B
ChR2 in DMH^GAD2
Jump (%)
n.s.
tdTom
ChR2
C
ChR2 in DMH^GAD2
Push-bedding (%)
***
tdTom
ChR2
D
TAC1
VGAT
DAPI
E
ChR2-mCherry in DMH^TAC1
F
Push-bedding
Self grooming
Rearing
Jumping
Tail rattling
Freezing
Duration (s) in 2 min
tdTom
ChR2
Push-bedding (%)
***
tdTom
ChR2
G
Pupil Size Z-score
Time (s)
Pupil Size Z-score
*
tdTom
ChR2
I
On
Off
Time in opto chamber (%)
*
tdTom
ChR2
H
Whisking Activity Z-score
Time (s)
Whisking Activity Z-score
*
Control
ChR2
J
ChR2 in DMH^TAC1
own nesting material
Opto ON inside and outside
Time inside home-like space (%)
**
tdTom
ChR2
K
ChR2 in DMH^TAC1
day 1 → day 2,3 → day 4
No opto
Opto
No opto
Push-bedding Duration (s)
*
Day1
Day4
L
stGtACR2 in DMH^TAC1
TMT
Outside stressor
Push-bedding Duration (s)
***
tdTom
stGtACR2
M
stGtACR2 in DMH^TAC1
TMT
Inside stressor
Number of Jumps
n.s.
tdTom
stGtACR2
N
LED/470nm
Photodetector/Amplifier
Dichroic mirror
Inside or outside stressor
O
Inside stressor
Outside stressor
***
Calcium activity (dF/F0 Zscore)
Time (s)
P
**
Mean Zscore
Inside stressor
Outside stressor

A

DIO-ChR2-mCherry in DMH^{TAC1}

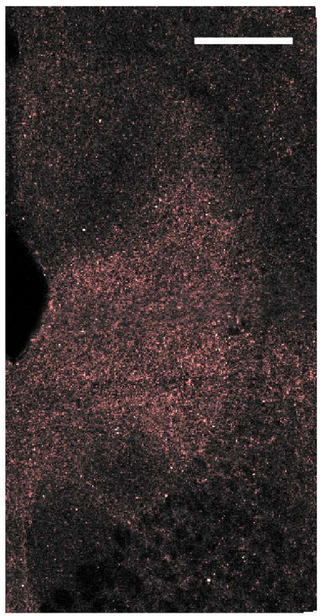

B

DIO-ChR2-mCherry in DMH^{VGluT2}

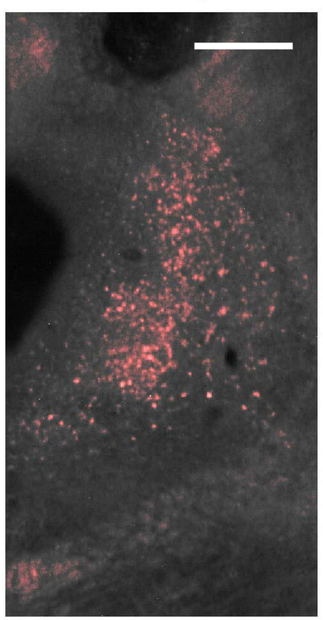

C

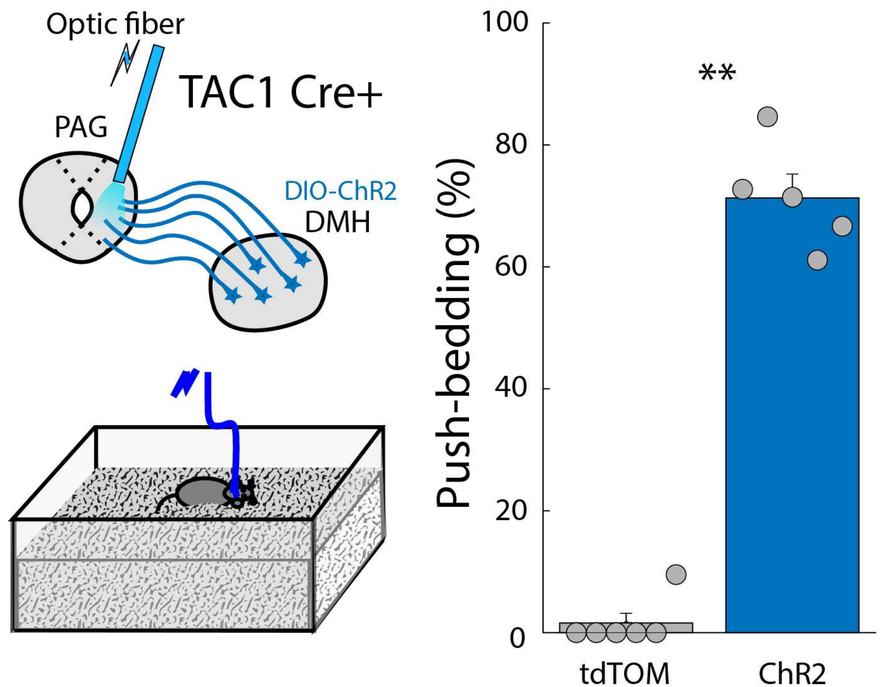

D

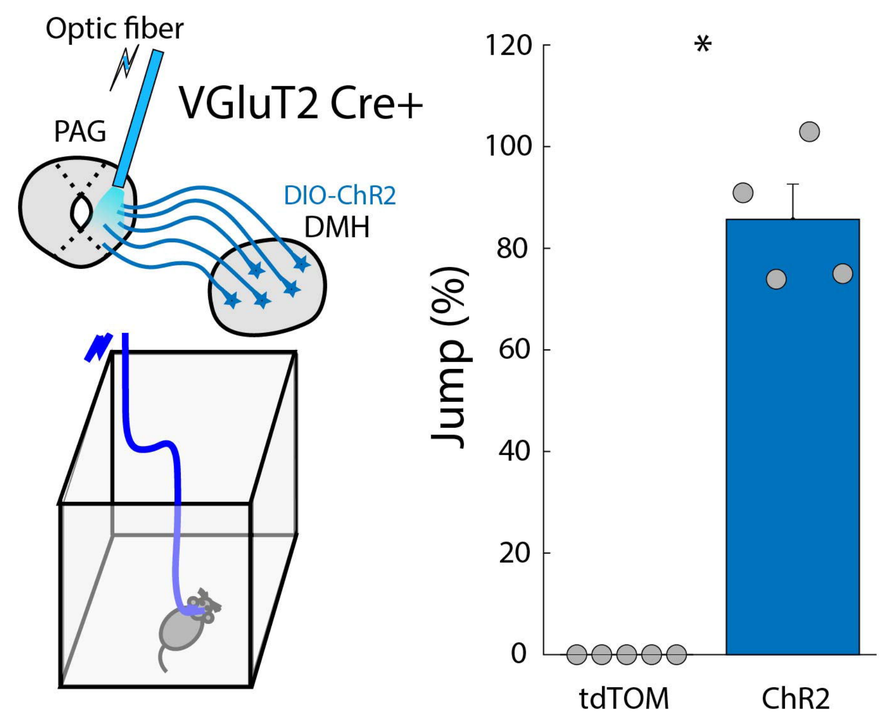

E

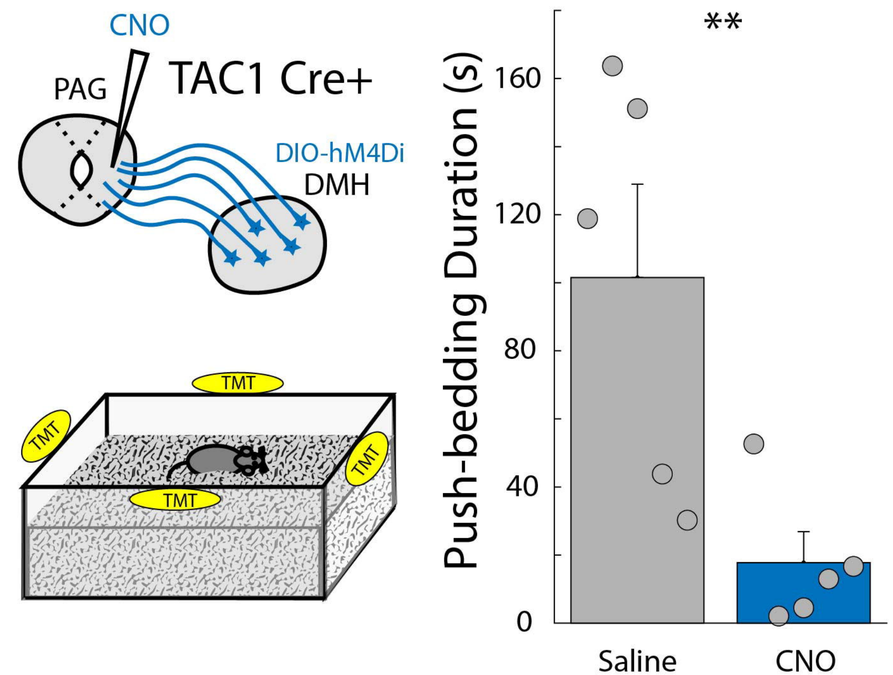
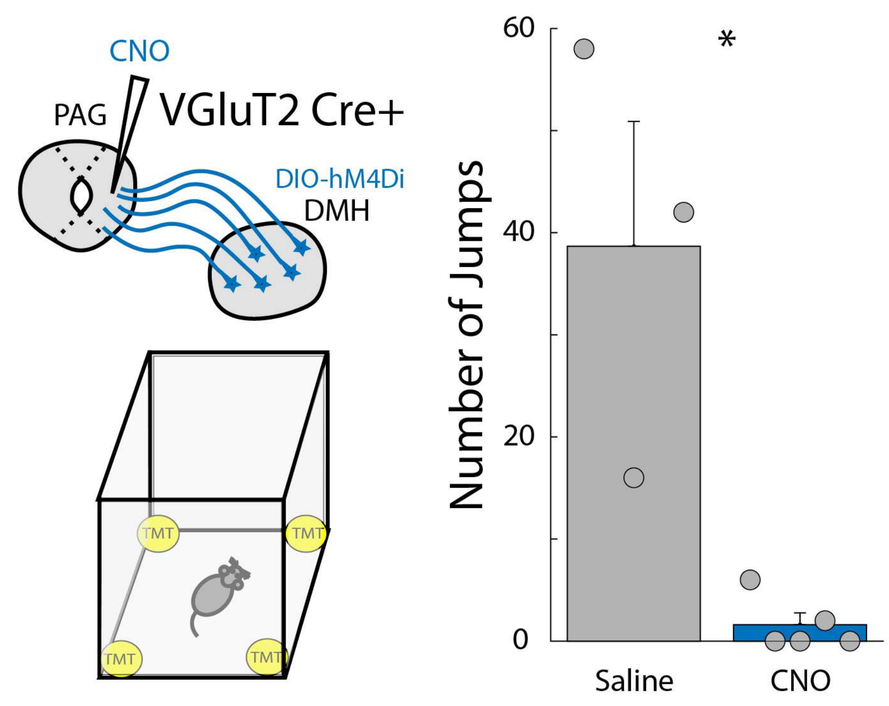
F